ASIIMETRIK
JURNAL ILMIAH REKAYASA DAN INOVASI
p-ISSN: 2655-1861, **e-ISSN:** 2716-2923
Volume **8** Number **2**, **2026**

Co-Design of Magnet-Edge One Step Slotting and Stator Dummy Slots to Reduce Cogging Torque and Unbalanced Magnetic Pull

Gita Wardhana[1], Tajuddin Nur[2]*, Lucio Alfredo Correia[3], Herlina[4], Maria Angela Kartawijaya[2]
[1]Master's Program in Electrical Engineering, Atma Jaya Catholic University of Indonesia, Jakarta, Indonesia
[2]Department of Electrical Engineering, Atma Jaya Catholic University of Indonesia, Jakarta, Indonesia
[3]Department of Electrical Engineering, Universidade Timor Lorosa'e, Timor Leste
[4]Department of Electrical Engineering, Sriwijaya University, South Sumatera, Indonesia

**Correspondence email*: *tans@atmajaya.ac.id*

Received: 14/05/2026 Revised: 28/05/2026 Accepted: 05/06/2026

Abstract: Low-speed wind generators require low cogging torque to ensure reliable start-up and low unbalanced magnetic pull to reduce vibration and bearing stress. This study examines a co-design approach that combines one-step magnet-edge slotting and stator dummy slots in a 24-slot/20-pole fractional-slot permanent magnet machine. Three configurations were analysed using two-dimensional finite element analysis in FEMM 4.2: the baseline model, the one-step magnet-edge slotting model, and the integrated one-step magnet-edge slotting + dummy-slot model. Cogging torque was calculated from Maxwell stress in the air gap, while unbalanced magnetic pull was evaluated through horizontal and vertical electromagnetic force components. The results show that one-step magnet-edge slotting reduces peak cogging torque by about 74.3% compared with the baseline model. The combined one-step magnet-edge slotting + dummy-slot design achieves a larger reduction of about 99.4%. This configuration also decreases unbalanced magnetic pull by approximately 92% on the X-axis and 90% on the Y-axis. When the unbalanced magnetic pull effect is included, the effective cogging-torque reduction remains about 98.9%. These findings indicate that integrating rotor-side magnet-edge slotting with stator-side permeance shaping provides an effective passive strategy for improving start-up performance and radial-force balance in low-speed permanent magnet wind generators.

Keywords: PMM; cogging-torque; UMP; OSS; dummy-slot

SDGs Problem Solving

This work contributes to SDG Chapter #7 by improving the reliability and efficiency of wind generators through the reduction of cogging torque and vibration, enabling sustainable, cleaner electricity generation and encouraging the adoption of small-scale renewable energy systems.

Jurnal Asiimetrik: Jurnal Ilmiah Rekayasa dan Inovasi - ASIIMETRIK is an open access and peer-reviewed journal published by Faculty of Engineering, Universitas Pancasila, Indonesia.

1. INTRODUCTION

Small permanent magnet generators must provide consistent torque at minimal rotating speeds, as the aerodynamic torque available during cut-in circumstances is constrained and subject to significant fluctuations (Abduh, Karunanithi and Nur, 2025). Cogging torque emerges as a significant impediment at low speeds due to the formation of a detent effect, even in no-load conditions, which elevates the starting threshold, exacerbates vibration, and diminishes power quality in small-scale renewable systems (Hao *et al.*, 2023). Researchers regard cogging torque not merely as a tweak, but as a fundamental limitation in the design of fractional-slot permanent magnet generator topologies aimed at low wind speed operation (Said, Nur and Herlina, 2024).

Cogging torque originates from the periodic variation of magnetic reluctance caused by slotting, magnet edges, and local saturation, so it scales with the interaction between airgap permeance harmonics and magnet flux harmonics (Hao *et al.*, 2023). Studies indicate that reducing torque ripple in permanent magnet machines requires alterations to the rotor (e.g., trimming edges, tuning pole arcs, or moving magnets), stator (e.g., adding auxiliary slots, dummy slots, or redesigning tooth tips), and electromagnetic optimization within manufacturability limits (Pranjić and Virtič, 2024). Both empirical and numerical results show that magnet-structure engineering is particularly effective for fractional-slot generators because it targets the main spatial harmonics that produce detent torque without redesigning the winding set (Said, Nur and Herlina, 2024). Other studies have shown that auxiliary-slot asymmetrical and pole-arc control considerably minimize cogging torque. If the design does not explicitly govern harmonic interactions, these two strategies may affect harmonic content and increase tolerance sensitivity (Wan *et al.*, 2022).

At the same time, generator reliability and vibration behavior depend on the radial force balance in the air gap. Unbalanced magnetic pull (UMP) appears when the radial electromagnetic forces become asymmetric due to eccentricity, rotor deflection, assembly tolerances, or magnetic asymmetry, and it can trigger extra bearing load, noise, and long-term mechanical wear (Zhu *et al.*, 2023). Analytical and numerical models confirm that eccentricity-related electromagnetic force components interact with rotor dynamics and can amplify vibration responses under operating conditions, so designers must evaluate force harmonics together with torque characteristics, not in isolation (Xu *et al.*, 2024). Evidence from machine-condition studies also shows that UMP-related phenomena can be critical in rotating energy conversion systems because they couple mechanical faults and electromagnetic nonuniformity through the air gap (Dawood *et al.*, 2025).

Notwithstanding the extensive literature on cogging torque, two significant gaps persist in scholarly contributions in generator-focused research. Many reductions strategy declare enhancements in cogging torque without concurrently measuring the resultant change in UMP, even though rotor-side changes can affect the radial force distribution and elevate the chance of force imbalance (Pranjić and Virtič, 2024). Second, the evidence base still concentrates heavily on traction motors, while fractional-slot surface-mounted permanent magnet generators intended for very low wind speed operation receive less systematic attention, especially for topology-specific designs such as 24-slot/20-pole configurations where harmonic interactions differ from common industrial motor slot–pole sets (Abduh, Karunanithi and Nur, 2025). These gaps limit design transferability because a low cogging torque solution is not automatically a low vibration risk solution when eccentricity and force asymmetry exist in real deployments (Huang *et al.*, 2025).

Although many studies have addressed cogging-torque reduction, a specific gap remains in generator-oriented applications. Most previous works report lower cogging torque after geometric modification but do not examine whether the same modification also changes the unbalanced magnetic pull (UMP). This issue is important because a rotor-side design change can reduce torque ripple while still affecting the radial force distribution in the air gap. Previous studies have also focused mainly on traction motors or general permanent magnet machine topologies (Said, Nur and Herlina, 2024). In contrast, fractional-slot surface-mounted permanent magnet generators for very low wind-speed operation have received less focused attention (Hao *et al.*, 2023). This gap is especially relevant for the 24-slot/20-pole topology because its slot–pole harmonic interaction differs from many common industrial motor configurations. Therefore, cogging torque and UMP need to be evaluated together to obtain a more complete assessment of the proposed design.

This study addresses the identified gap by analysing a 24-slot/20-pole fractional-slot surface-mounted permanent magnet generator for low-speed wind-energy applications. The baseline design is compared with two modified configurations: a one-step magnet-edge slotting (OSS) model and a combined OSS + stator dummy-slot model. The OSS structure is applied to reduce flux concentration at the magnet edge and smooth the effective airgap permeance, which is expected to weaken the dominant cogging-torque harmonics. The stator dummy slots are added to further suppress the remaining slotting-related permeance harmonics and improve radial-force symmetry (Zhao *et al.*, 2025).Under the same stator and winding constraints, the combined configuration is expected to provide better cogging torque and UMP reduction than rotor-side modification alone (Strączyński, Różowicz and Baran, 2025).

The proposed configurations are evaluated using two-dimensional finite element analysis in FEMM 4.2 under no-load rotor-position sweep conditions. The simulation extracts the air-gap field quantities needed to calculate cogging torque and UMP, allowing the torque and force responses of each design variant to be compared before prototype development.

The objectives of this study are to quantify the cogging-torque reduction achieved by the OSS and OSS + stator dummy-slot configurations, evaluate the corresponding changes in UMP components, and explain the relationship between geometric modification, air-gap field distribution, torque ripple, and radial-force balance. The main contribution of this work lies in the simultaneous evaluation of cogging torque and UMP in a 24-slot/20-pole low-speed permanent magnet generator. This study offers a passive geometric design strategy that can support reliable start-up and reduce vibration risk in low-speed wind-generator applications (Pranjić and Virtič, 2024).

2. METHODOLOGY

This study was conducted through a structured finite-element-based procedure to evaluate the effect of one-step magnet-edge slotting and stator dummy slots on cogging torque and unbalanced magnetic pull in a 24-slot/20-pole fractional-slot permanent magnet machine. The research procedure began with the definition of the baseline machine, followed by the development of the investigated configurations, finite element modelling in FEMM 4.2, air-gap field extraction, cogging torque calculation, UMP calculation, and comparative performance analysis. The overall research workflow is presented in Figure 1. As shown in Figure 1, the analysis started by defining the baseline machine geometry, material properties, and operating assumptions. Three configurations were then prepared: the baseline model, the one-step magnet-edge slotting (OSS) model, and the integrated OSS + stator dummy-slot model. Each model was simulated under the same no-load rotor-position sweep using FEMM 4.2 and LUA-based automation. The normal and tangential air-gap flux-density components were extracted using five dummy lines across the air-gap region. These field data were used to calculate cogging torque through Maxwell stress formulation and to evaluate the horizontal and vertical UMP components. The simulation was repeated when the configuration did not meet the expected performance trend. The final comparison was made based on peak cogging torque, cogging-torque reduction, UMP response, and the identification of the most effective passive configuration for low-speed wind-generator operation.

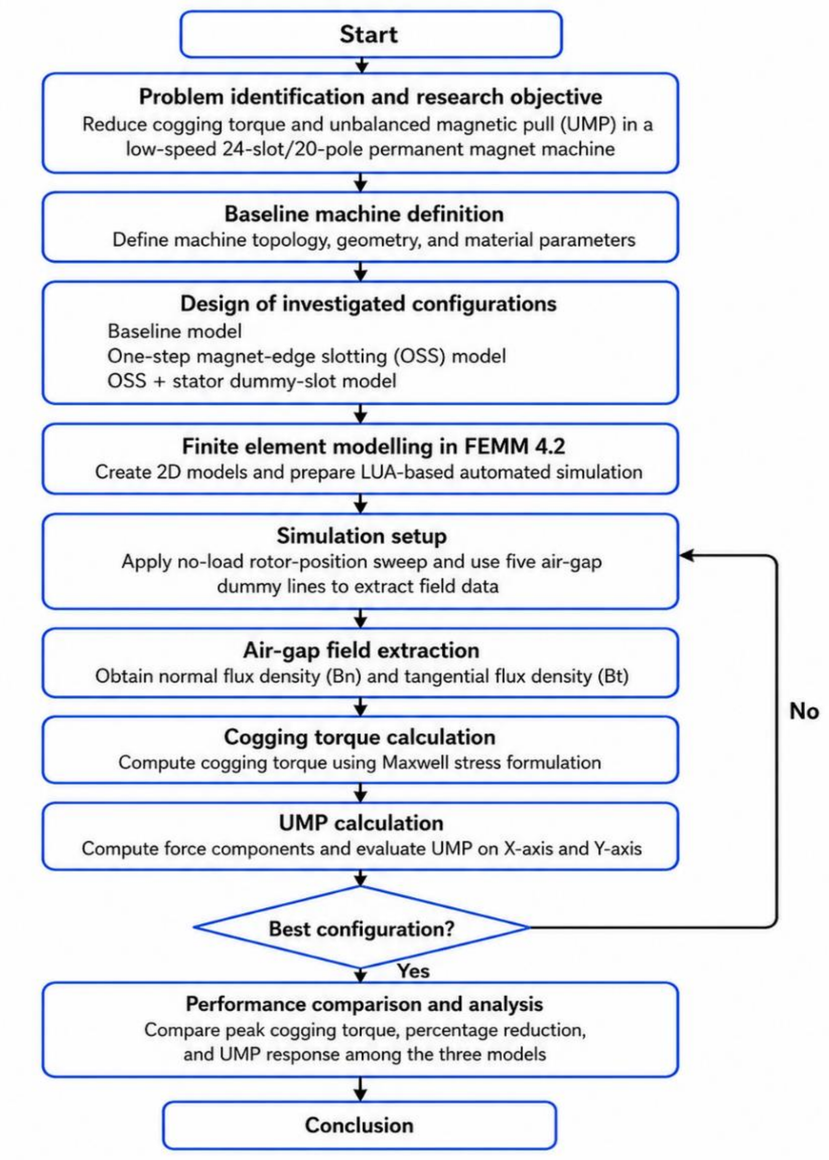

Figure 1. Research flowchart

2.1. Materials and Studied Machine

This study focuses on a permanent magnet machine (PMM) intended for low-speed wind-energy applications, where the prime mover often delivers limited starting torque and fluctuates with wind speed. The investigated topology uses a fractional-slot-number (FSN) configuration with 24 stator slots and 20 poles, as illustrated in Figure 2.

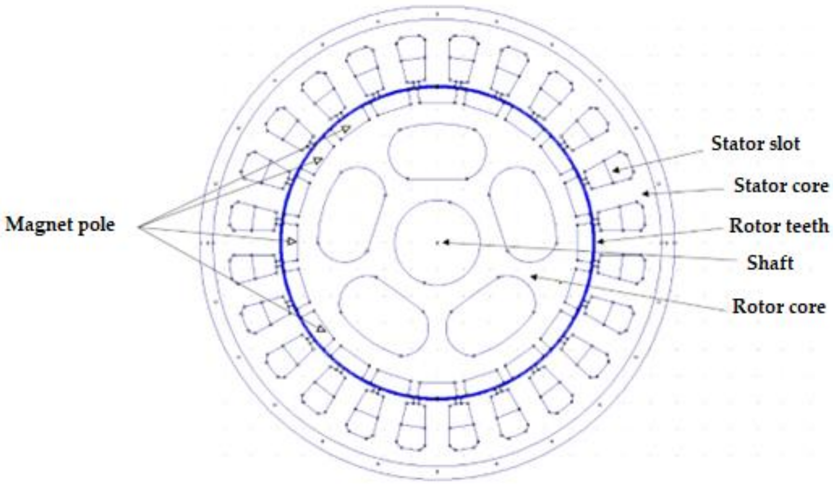

Figure 2. Basic construction of Permanent Magnet Machines 24 slots and 20 poles

FSN machines commonly show lower cogging torque than integral-slot-number designs, yet they can exhibit stronger radial force asymmetry that drives unbalanced magnetic pull (UMP). Cogging torque (CT) is significant in wind turbines as it impedes rotor movement at rest and can halt the machine during low-wind conditions. The concentration of flux at the magnet tips frequently exacerbates CT harmonics; hence, numerous recent studies focus on magnet-edge shaping or pole-edge modification to mitigate CT (Yan *et al.*, 2024).

2.2. Design Variants and Mitigation Strategy

The method evaluates three PMM constructions that differ only in rotor–stator geometric features that influence airgap permeance and local flux-density harmonics:

- Baseline model (reference geometry).
- One-step magnet-edge slotting model, which modifies the magnet edge to weaken tangential flux-density peaks linked to CT.
- Combined model that integrates magnet-edge modification with stator dummy slots on selected tooth regions to reshape the effective permeance distribution and suppress CT components.

Dummy-slotting belongs to stator-side geometric approaches that reduce cogging torque by changing local permeance without changing winding layout.

2.3. Finite-Element Model and Evaluation

This research implemented a two-dimensional finite-element model of the PMM and solved the magnetic field over one electrical period by stepping into the rotor position. All configurations are evaluated using two-dimensional electromagnetic finite-element analysis in Finite Element Method

Magnetics (FEMM) version 4.2. The study extracted air-gap flux density using multiple sampling lines (dummy lines) distributed across the air-gap region to stabilize numerical integration of stress-based quantities. The model uses five dummy lines, where the first line aligns with the tooth-tip region and the remaining lines span the air gap to capture both radial and tangential field components. To accelerate parametric studies, FEMM is coupled with LUA scripting, so simulations run iteratively and consistently across design variants. This automation approach is consistent with recent FEMM-based machine-design workflows that integrate scripting for repeatability and batch analysis. Recent study employs FEM-based field sampling to quantify alterations in CT arising from modifications to magnet-edge and slot shape (Abduh, Karunanithi and Nur, 2025).

2.4. Cogging Torque Formulation

Cogging torque originates from the interaction between the rotor's permanent-magnet field and the spatial variation of stator permeance (Yan *et al.*, 2024). We computed CT using the Maxwell-stress approach in the air gap by integrating the product of radial and tangential flux-density components along a circular path (Hosseinpour *et al.*, 2024):

$$T_c = \frac{L_{stk}}{\mu_0} \int_0^{2\pi} r^2 \, B_n \, B_t d\theta \qquad (1)$$

where:

l_{stk} = stack length,

r = the radius of the integration path,

μ_0 = the permeability of free space,

B_n = radial flux density, and

B_t = tangential flux density.

This stress-based formulation is widely used in recent PM-machine CT studies that rely on air-gap field components from FEM (Li *et al.*, 2024). To interpret why dummy slots, reduce CT, we used the standard air-gap reluctance approximation:

$$R_g = \frac{l_g}{\mu_0 A_g} \qquad (2)$$

A is the effective area of the flux path. Dummy slots reduce the effective tooth area locally, which alters the permeance waveform and can reduce CT driving harmonics in the tangential stress component.

2.5. Unbalanced Magnetic Pull Formulation

UMP appears when the radial magnetic forces do not cancel, which commonly happens under eccentricity or asymmetric field distribution. The author computed the Cartesian force components from Maxwell stress along the same air-gap integration path (Nur, Suherman and Wahab, 2021).

$$F_t = \frac{1}{\mu_0}(B_n B_t) \cos\theta \qquad (3)$$

$$F_n = \frac{1}{2\mu_0}(B_n^2 - B_t^2) \sin\theta \qquad (4)$$

$$F_x = f_n \cos\theta - f_t \sin\theta \qquad (5)$$

$$F_y = f_n \sin\theta + f_t \cos\theta \quad (6)$$

where:

F_t = tangential magnetic force (N)
F_n = normal magnetic force (N)
F_x = horizontal unbalanced magnetic pull (N)
F_y = vertical unbalanced magnetic pull (N)

This approach aligns with recent PM-machine studies that calculate unbalanced magnetic force via stress integration to quantify force growth under eccentricity and geometry changes (Kim *et al.*, 2020).

2.6. Performance Evaluation Metrics

After the cogging torque and unbalanced magnetic pull components were obtained from the finite-element results, the performance of each configuration was evaluated using the baseline model as the reference. The main performance indicator was the percentage reduction in peak cogging torque, which was calculated by comparing the peak cogging torque of the modified model with that of the baseline model. The cogging torque reduction is expressed as (Ling and Nur, 2016; Nur and Mawar, 2020; Nur, Suherman and Wahab, 2021):

$$T_c\ (\%) = \left(100\ \% - \frac{T_{c2}}{Tc1}\ x\ 100\%\right) \quad (7)$$

where T_{c1} is the peak cogging torque of the original permanent magnet machine, and T_{c2} is the peak cogging torque obtained from the OSS model or the integrated OSS + stator dummy-slot model.

The same comparison principle was applied to evaluate the reduction of unbalanced magnetic pull. The horizontal and vertical force components were compared with the corresponding baseline values to determine whether the proposed geometric modification reduced radial-force imbalance. The final assessment was based on three indicators: peak cogging torque, cogging-torque reduction percentage, and UMP reduction on the X-axis and Y-axis. This evaluation procedure ensures that the selected configuration does not only reduce cogging torque but also improves magnetic-force balance in the air gap.

3. RESULTS AND DISCUSSION

This section evaluates a fractional-slot permanent magnet machine (24 slots/20 poles) with three rotor–stator configurations, namely a conventional baseline (original), a one-step slotting of the magnet-edge model (OSS), and a combined magnet-edge one step slotting and stator dummy-slot model using the same core, winding, and operating assumptions as defined before.

3.1. Electromagnetic Field Distribution for the Three Models

The three rotor configurations keep the same machine core and winding set, so any change in torque ripple and lateral force must come from how the rotor-side magnet geometry reshapes the air-gap field (Abduh, Karunanithi and Nur, 2025). The flux maps (Figure 3) show comparable main flux paths through the stator teeth and back-iron, while the local field around the magnet edges changes visibly when edge slotting and the dummy-slot concept are applied.

This observation supports an important point: core flux-density magnitude alone does not explain the cogging-torque trend, because the torque ripple mechanism depends on the air-gap stress harmonics rather than the bulk flux level in the yokes. To connect field features to torque, the analysis uses the Maxwell-stress form in which cogging torque is proportional to the product of the normal and tangential air-gap flux-density components (Hosseinpour *et al.*, 2024). The procedure extracts Bn and Bt along several dummy lines in the air gap to capture how the slot opening and magnet edges modulate the field.

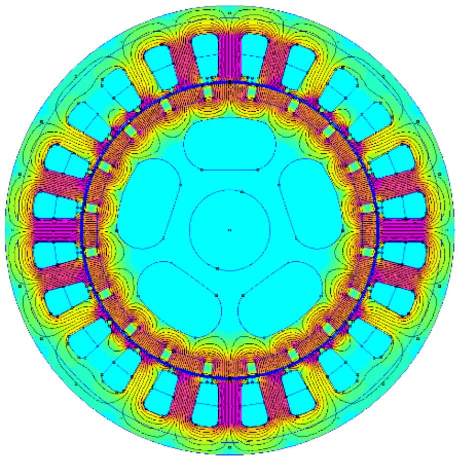

(a). Baseline model

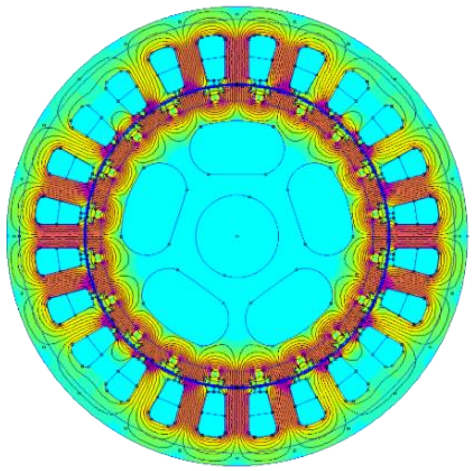

(b). OSS model

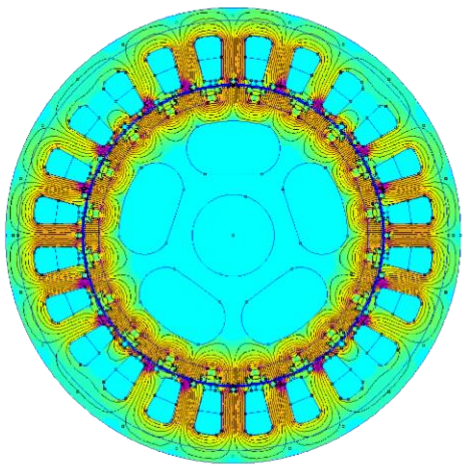

(c). Combine model (OSS + dummy slot stator)

Figure 3. Magnetic flux distribution of the investigated permanent magnet machine of the three designs

In this framework, Bt acts as the direct torque-ripple carrier because the tangential stress term scales with BnBt, so any design feature that suppresses Bt around magnet edges and slot openings will reduce cogging torque. Recent studies also stress that reducing the tangential component near the magnet edge is an efficient lever for lowering peak cogging torque, especially when geometric constraints limit the use of full skewing. The magnetic flux distribution of the three models can be seen in Figure 3.

Across the three models, the electromagnetic implication is consistent and specific. In Figure 3(a), the original rotor creates a stronger edge-related permeance variation, which increases local tangential field distortion at the air gap. Figure 3(b), the one-step magnet-edge slotting (OSS) reduces the abruptness of the magnet-edge interaction with the stator slotting, so it reduces the local tangential component that feeds torque ripple. And the Figure 3(c), combination model of OSS and the dummy-slot configuration go further by adding a stator-side permeance shaping element and by lowering the pole-arc coefficient (from 0.9 to 0.8), which smooths the slot–pole alignment effect and weakens the dominant permeance harmonics that generate cogging torque. This field redistribution is consistent with the broader literature that reports large cogging-torque reductions when dummy-slotting is combined with magnet-edge shaping, because the combined geometry attacks both the slotting permeance ripple and the tangential flux pathway.

3.2. Cogging Torque Reduction Performance

The cogging-torque performance of the three configurations was evaluated using the procedure described in the methodology section. The peak cogging torque of each modified model was compared with the baseline model to determine the reduction level. The quantitative comparison is presented in Table 1.

Table 1. Peak of the cogging torque and the reduction

Configuration	Peak of cogging torque (N.m)	Relative reduction vs baseline
Baseline	0.0053733	0.533
OSS	0.0013790	74.34%
OSS + Dummy	0.0000319	99.41-99.42%

The original comparison plot can be seen in Figure 4; it directly visualizes the peak-to-peak reduction trend across the three designs.

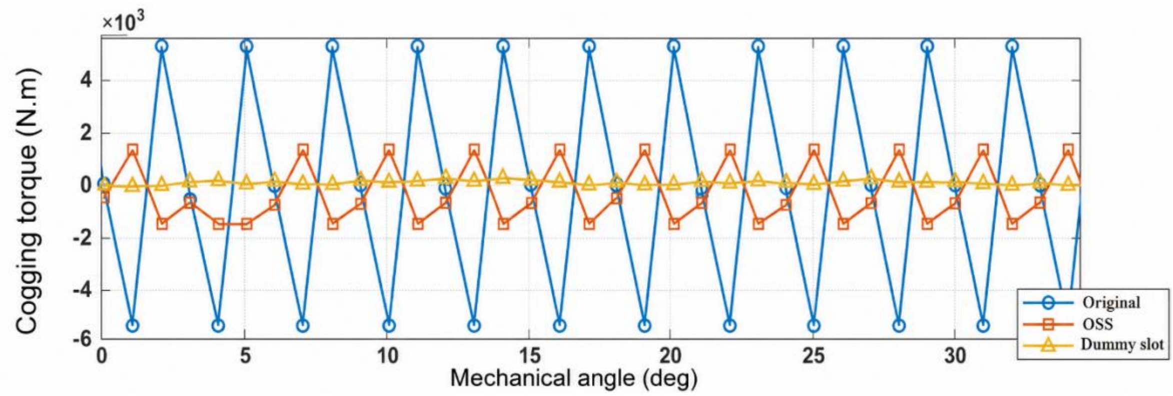

Figure 4. Comparison of cogging torque among the three investigated designs

Figure 4 compares the cogging-torque (CT) waveforms for the three permanent-magnet machine (PMM) configurations investigated. The baseline (original) design produced the highest CT peak, equal to 0.0053733 N·m, which indicates strong tangential interaction between magnet edges and stator slots. After applying one-step magnet slotting (OSS) at both magnet ends, the CT peak decreased to 0.0013790 N·m. This reduction confirms that reshaping the magnet-edge region reduces the tangential flux component that couples with the slot-opening permeance variation.

This trend aligns with recent studies showing that small geometric changes at the pole edge (or effective pole-arc/pole-pitch adjustment) can reduce CT by weakening slot-related air-gap field modulation.

The third design integrates OSS and a stator dummy slot. The CT peak dropped further to 0.0000319 N·m, corresponding to a 99.41–99.42% reduction relative to the baseline. The mechanism is consistent with the stated design rationale: dummy slots increase the effective air-gap area without changing the physical air-gap distance, which reduces air-gap reluctance and suppresses the slotting-driven torque component (Yan *et al.*, 2024). The result is also consistent with recent PM-generator work that reports strong CT mitigation when magnet structure engineering is combined with slot-side or permeance-shaping measures.

3.3. Unbalanced Magnetic Pull Response (UMP_x and UMP_y)

This research evaluates unbalanced magnetic pull using airgap "dummy lines" and resolves it into the x-axis and y-axis force components, then compares the three configurations over rotor position as shown in Figure 5 and Figure 6.

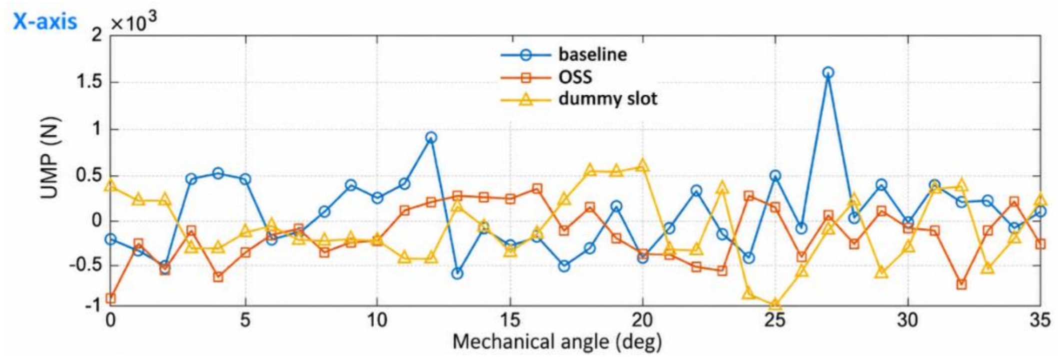

Figure 5. Comparison of UMP on X-axis against the three models

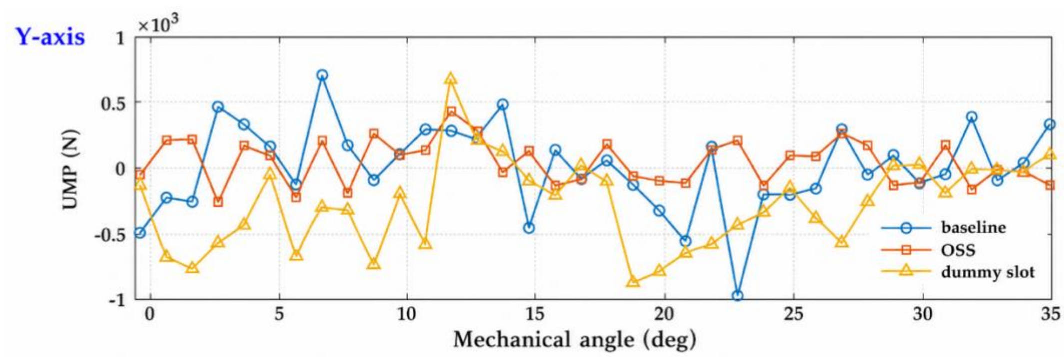

Figure 6. Comparison of UMP on Y-axis against the three models

Figure 5 and Figure 6 show the UMP components versus mechanical rotor angle. The dummy-slot configuration reduces UMP by about 90% in the vertical direction and 92% in the horizontal direction relative to the original design. This reduction indicates that the combined geometric changes do not only suppress torque ripple; they also improve circumferential symmetry of the air-gap field, which reduces the net lateral force produced by uneven air-gap stress.

The same linkage between air-gap flux-density asymmetry, Maxwell stress, and unbalanced force appears in recent modelling work on eccentricity and UMP, which explicitly uses stress-based formulations and relates flux-density modulation to unbalanced pull and vibration features (Song *et al.*, 2024).

A key robustness result appears when UMP is accounted for in the torque-reduction evaluation. The cogging-torque reduction decreases from 99.42% to 98.87% when UMP effects are included, but the mitigation remains dominant and practically significant. This behaviour is technically expected: once the design suppresses the main slot-pole energy variation, residual asymmetries (including small force-related field distortions) can become a larger share of the remaining ripple. Recent studies on eccentricity faults in PMSMs report that eccentricity-induced asymmetry increases UMP and can accelerate vibration and mechanical aging, so designs that reduce UMP can improve operational stability even when average electromagnetic performance already looks acceptable (Mortezaei, Aliabadi and Javadi, 2024).

Compared with prior reports, the >90% UMP reduction is competitive for a method that does not rely on heavy mechanical skewing or added active control (Zhu *et al.*, 2023). Recent work also emphasizes that UMP can arise not only from eccentricity but also from field-harmonic interactions and post-fault operating modes, which strengthens the value of passive geometric symmetry improvements (Drobnič and Fišer, 2025). The present trend—simultaneous reduction of cogging torque and UMP—matches broader findings that link flux-density modulation to both torque ripple and unbalanced magnetic forces in permanent-magnet machines.

Table 2. Summary of cogging torque and UMP performance

Metric	Baseline	OSS	OSS + Dummy slot
Peak CT (N.m)	0.0053733	0.0013790	0.0000319
CT reduction vs baseline (%)	-	74.34	99.41
UMP reduction on X-axis vs baseline (%)	-	Reduced	92%
UMP reduction on Y-axis vs baseline (%)	-	Reduced	90%
CT reduction incl UMP effect (%)	-	-	98.87%

Table 2 presents the final quantitative comparison of the three models. The table highlights the magnitude of cogging-torque suppression and the corresponding improvement in radial-force balance, which are the two primary targets for low-speed wind operation.

Overall, the results establish a clear field–stress–performance link: the modifications reshape the air-gap flux-density components (Bn and Bt), which directly suppresses cogging torque and improves radial-force balance. The combined OSS–dummy-slot design delivers the most consistent improvement across both metrics and remains robust when UMP-related disturbance is considered, positioning the proposed geometry as a practical, competitive solution relative to recent cogging-torque and UMP mitigation studies.

4. CONCLUSION

This study examined the influence of one-step magnet-edge slotting (OSS) and stator dummy slots on cogging torque and unbalanced magnetic pull (UMP) in a 24-slot/20-pole fractional-slot permanent magnet machine for low-speed wind-generator applications. The results indicate that

OSS can reduce cogging torque, while the combined OSS + stator dummy-slot configuration provides the strongest overall improvement. The combined design weakens the dominant slot–pole interaction and improves radial-force balance, showing that rotor-side magnet-edge modification and stator-side permeance shaping can complement each other as a passive mitigation strategy.

The main finding is that cogging torque and UMP can be reduced simultaneously through coordinated geometric modification without changing the main stator and winding structure. This result is relevant for low-speed wind generators because lower cogging torque supports easier start-up, while lower UMP helps reduce vibration tendency and bearing stress. This study is limited to two-dimensional finite element analysis under no-load conditions.

Future work should include prototype testing, load-condition analysis, manufacturing-tolerance evaluation, and eccentricity sensitivity analysis. Experimental validation is also required to confirm whether the simulated improvements can be maintained under practical low-speed wind-generator operation.

REFERENCES

Abduh, S., Karunanithi, S. and Nur, T. (2025) 'Analysis of the Cogging Torque Reduction in Permanent Magnet Generators for a Very Low Wind Speed', *Energies*, 18(11), p. 2802. Available at: https://doi.org/10.3390/en18112802.

Dawood, A. *et al.* (2025) 'Improved Performance of Single Sided Axial Flux for Reduction in Cogging Torque (IMPACT)', *Results in Engineering*, 25, p. 103778. Available at: https://doi.org/10.1016/j.rineng.2024.103778.

Drobnič, K. and Fišer, R. (2025) 'Unbalanced Magnetic Pull in an 18-Slot/8-Pole Dual Three-Phase Machine Under Different Modes of Operation', *COMPEL - The international journal for computation and mathematics in electrical and electronic engineering*, 44(3), pp. 274–289. Available at: https://doi.org/10.1108/COMPEL-09-2024-0402.

Hao, W. *et al.* (2023) 'Methods for Reducing Cogging Force in Permanent Magnet Machines: A Review', *Energies*, 16(1), p. 422. Available at: https://doi.org/10.3390/en16010422.

Hosseinpour, A. *et al.* (2024) 'Calculating Torque, Back-EMF, Inductance, And Unbalanced Magnetic Force for a Hybrid Electrical Vehicle by In-Wheel Drive Application', *Scientific Reports*, 14(1), p. 12912. Available at: https://doi.org/10.1038/s41598-024-63702-8.

Huang, C. *et al.* (2025) 'Research on Cogging Torque Reduction Based on Multi-Parameter Optimization of Auxiliary Slots and Pole-Arc Coefficient', *Journal of Electrical Engineering & Technology*, 20(3), pp. 1439–1449. Available at: https://doi.org/10.1007/s42835-024-02058-5.

Kim, H. *et al.* (2020) 'Unbalanced Magnetic Pull Analysis for Rotordynamics of Induction Motors', *2020 International Conference on Electrical Machines (ICEM)*. *2020 International Conference on Electrical Machines (ICEM)*, Gothenburg, Sweden: IEEE, pp. 2469–2475. Available at: https://doi.org/10.1109/ICEM49940.2020.9270865.

Li, Zhihua *et al.* (2024) 'Calculation and Analysis of Unbalanced Magnetic Pull Caused by Rotor Eccentricity Based on No-Load Characteristics', *The Proceedings of the 18th Annual Conference of China Electrotechnical Society*. *The 18th Annual Conference of China Electrotechnical Society*, Singapore: Springer Nature, pp. 356–370. Available at: https://doi.org/10.1007/978-981-97-1447-6_38.

Ling, J.M. and Nur, T. (2016) 'Influence of Edge Slotting of Magnet Pole with Fixed Slot Opening Width on The Cogging Torque in Inset Permanent Magnet Synchronous Machine', *Advances in Mechanical Engineering*, 8(8), p. 1687814016659598. Available at: https://doi.org/10.1177/1687814016659598.

Mortezaei, S.R., Aliabadi, M.H. and Javadi, S. (2024) 'Eccentricity Fault Detection in Surface-Mounted Permanent Magnet Synchronous Motors by Analytical Prediction, FEM Evaluation, And Experimental Magnetic Sensing of The Stray Flux Density', *Journal of Magnetism and Magnetic Materials*, 589, p. 171441. Available at: https://doi.org/10.1016/j.jmmm.2023.171441.

Nur, T. and Mawar, S. (2020) 'Improvement of Cogging Torque Reduction by Combining the Magnet Edge Shaping and Dummy Slot in Stator Core of Fractional Slot Number in Permanent Magnet Machine', *IOP Conference Series: Materials Science and Engineering*, 807(1), p. 012023. Available at: https://doi.org/10.1088/1757-899X/807/1/012023.

Nur, T., Suherman, Y. and Wahab, H. (2021) 'The Effect of Magnet Structure on the Cogging Torque Reduction in a Permanent Magnet Generator', *Journal of Southwest Jiaotong University*, 56(1), pp. 313–323. Available at: https://doi.org/10.35741/issn.0258-2724.56.1.29.

Pranjić, F. and Virtič, P. (2024) 'Cogging Torque Reduction Techniques in Axial Flux Permanent Magnet Machines: A Review', *Energies*, 17(5), p. 1089. Available at: https://doi.org/10.3390/en17051089.

Said, S.M., Nur, T. and Herlina, H. (2024) 'The Application of Magnet Structures to Reduce the Cogging Torque Associated with Fractional Slot Number in Permanent Magnet Generators', *Energies*, 17(11), p. 2505. Available at: https://doi.org/10.3390/en17112505.

Song, Y. *et al.* (2024) 'Research on Unbalanced Characteristics of Axial-Varying Eccentric Rotor Based on Signal Demodulation', *Mechanical Systems and Signal Processing*, 220, p. 111647. Available at: https://doi.org/10.1016/j.ymssp.2024.111647.

Strączyński, P., Różowicz, S. and Baran, K. (2025) 'Automated Laboratory Stand for Determining the Cogging Torque of a Small Permanent Magnet Electric Machine Using the MATLAB Environment', *Energies*, 18(5), p. 1047. Available at: https://doi.org/10.3390/en18051047.

Wan, X. *et al.* (2022) 'Minimization of Cogging Torque for V-Type IPMSM by the Asymmetric Auxiliary Slots on the Rotor', *IEEE Access*, 10, pp. 89428–89436. Available at: https://doi.org/10.1109/ACCESS.2022.3201246.

Xu, M.-X. *et al.* (2024) 'A Comprehensive Study on Electromagnetic Torque and Rotor UMP Based on An Improved 3D Static Air-Gap Eccentricity Model', *Alexandria Engineering Journal*, 105, pp. 370–380. Available at: https://doi.org/10.1016/j.aej.2024.06.088.

Yan, D. *et al.* (2024) 'Research on Cogging Torque Reduction Method for Permanent Magnet Synchronous Motor Accounting for The Magnetic Pole Edge Effect', *IET Electric Power Applications*, 18(1), pp. 64–75. Available at: https://doi.org/10.1049/elp2.12367.

Zhao, X.-K. *et al.* (2025) 'Axial Flux Permanent Magnet Synchronous Motor Cogging Torque Calculation Method Based on Harmonic Screening', *Energies*, 18(14), p. 3779. Available at: https://doi.org/10.3390/en18143779.

Zhu, R. *et al.* (2023) 'Calculation and Analysis of Unbalanced Magnetic Pull of Rotor under Motor Air Gap Eccentricity Fault', *Sustainability*, 15(11), p. 8537. Available at: https://doi.org/10.3390/su15118537.